Journal of Molecular Structure, 176 (1988) 33–60
Elsevier Science Publishers B.V., Amsterdam — Printed in The Netherlands

VIBRATIONAL SPECTRA OF *TRANS,TRANS*-1,2,3,4-TETRACHLORO-1,3-BUTADIENE; AND THE MOLECULAR STRUCTURE OF *TRANS,TRANS*-1,2,3,4-TETRACHLORO-1,3-BUTADIENE AND OF HEXACHLORO-1,3-BUTADIENE (A REINVESTIGATION) DETERMINED BY GAS-PHASE ELECTRON DIFFRACTION

GRETE GUNDERSEN, CLAUS J. NIELSEN and HANNE G. THOMASSEN*
Department of Chemistry, University of Oslo, Box 1033-Blindern, N-0315 Oslo 3 (Norway)
GEORG BECHER
National Institute of Public Health, Geitmyrsveien 75, N-0462 Oslo 4 (Norway)

(Received 29 September 1987)

ABSTRACT

Recorded infrared and Raman spectral data for *trans,trans*-1,2,3,4-tetrachloro-1,3-butadiene were interpreted in terms of C_2 molecular symmetry. Force-fields established on the basis of these data and literature spectral data for hexachloro-1,3-butadiene were used to calculate vibrational amplitude quantities and correction terms introduced in the structure analyses of the gas-phase electron-diffraction data. The geometrical parameters (r_a, $\angle_\alpha$) were for *trans,trans*-1,2,3,4-tetrachloro-1,3-butadiene: r(C–H) = 110.0(fixed), r(C=C) = 134.3(5), r(C–C) = 148.1(8), r(C–Cl) = 172.5(3) pm, $\angle$(C1=C2–C3) = 125.7(4), $\angle$(C3–C2–Cl) = 115.6(4), $\angle$(C2=C1–Cl) = 122.4(5), $\angle$(C2=C1–H) = 124.0(fixed) and ϕ(C=C–C=C) = 76.6(23)°; and for hexachloro-1,3-butadiene: r(C–Cl) = 171.6(3), r(C=C) = 134.1(5), r(C–C) = 148.5(9)pm, $\angle$(C1=C2–C3) = 122.6, $\angle$(C3–C2–Cl) = 115.8(4), $\angle$(C2=C1–Cl) = 122.50(10), $\angle$(C2=C1–C17) – $\angle$(C2=C1–C16) = –0.9(6) and ϕ(C=C–C=C) = 89(3)°. The last set of parameters is consistent with previously published GED results, with the exception of the torsional angle which was found to be sensitive to assumptions and refinements of vibrational amplitude quantities. The C=C–C=C root-mean-square torsional angle amplitudes (δ) and torsional angles (ϕ) determined by dynamic models of the molecules were δ = 16.3(16)° and ϕ = 77.8(20)°; and δ = 12.0(14)° and ϕ = 83.5(19)°.

Molecular mechanics calculations confirmed the *synclinal* conformations of the molecules and a wider torsional potential (larger δ-value) for the tetrachloro derivative which was also found to have lower torsional barriers than hexachloro-1,3-butadiene.

INTRODUCTION

Gas-phase electron diffraction (GED) investigations have recently shown that the gas of 2,3-dichloro- and of *cis,cis*-1,4,dichloro- 1,3-butadiene (here-

*Address correspondence to this author.

0022-2860/88/$03.50

after referred to as D23 and CC2, respectively) contain small amounts of a *gauche* form (ϕ(C=C–C=C), 50 to 60°) in addition to the prevailing *anti* conformer (ϕ=180°) [1,2]. Steric interactions prevent D23 and CC2 (*cis* refers to C1(4)–Cl and C2–C3) from assuming planar *syn* conformations (Fig. 1). By perchlorination also the *anti* form suffers from severe repulsions between substituents in the 1 and 3 positions of the butadiene skeleton (see Fig. 1), and hexachloro-1,3-butadiene (hereafter referred to as HEX) is found by GED to exist in a *synclinal* conformation with ϕ=78(1)° [3]. Similarly, only one non-planar form of gaseous hexafluoro-1,3-butadiene (ϕ=47(2)°) has been identified [4]. GED studies have also been performed for the three isomers of 3,4-dimethyl-2,4-hexadiene [5], which in the present context is more conveniently named 1,2,3,4-tetramethyl-1,3-butadiene and referred to as TME. Only *cis,cis* TME (*cis* refers to C1(4)–CH_3 and C2(3)–CH_3) has no particular steric repulsions in the planar *anti* conformation, and it is found to prevail in this form [5] which is also the conformation of *cis,cis*-1,2,3,4-tetrachloro-1,3-butadiene (ZZ4) in the solid state [6]. In contrast, the two other isomers of TME are both found to assume *synclinal* conformations with ϕ-values about 66° [5].

The non-planarity of highly substituted 1,3-butadienes has also been demonstrated in solution by ^{1}H NMR spectroscopy. Such dienes are chiral and consist of two enantiomers which may interconvert by partial rotation about the central single bond (Fig. 1). The barriers to enantiomerization for various

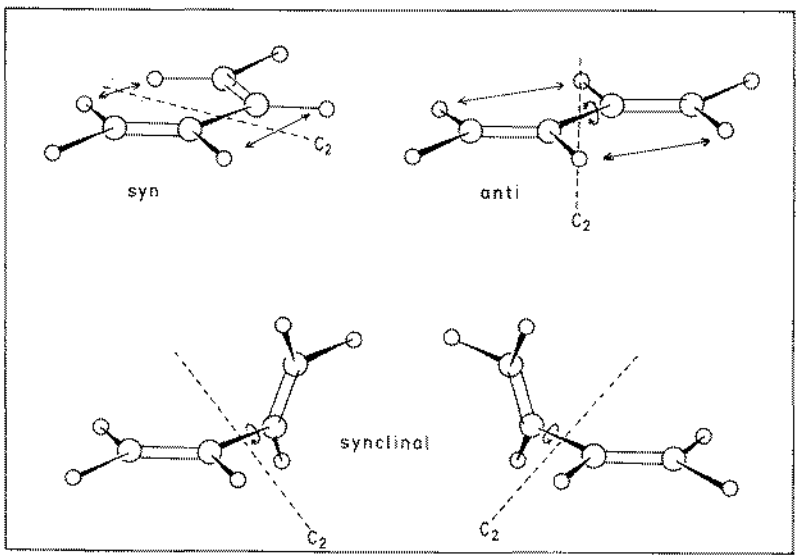

Fig. 1. The planar *syn* and *anti* conformations of 1,3-butadienes showing the possible interactions between substituents in 1,4 and 2,3 for *syn* and 1,3(2,4) for *anti*; and the two enantiomeric *synclinal* forms.

substituted *trans,trans*-1,2,3,4-tetrachloro-1,3-butadienes have been determined by dynamic NMR measurements using diastereotopic protons [7,8].

In the present paper we report the results of a GED study of *trans,trans*-1,2,3,4-tetrachloro-1,3-butadiene (hereafter denoted EE4) which as *trans,trans* TME and HEX, cannot possess *syn* or *anti periplanar* conformations due to steric repulsions between substituents.

Vibrational spectral data have also been recorded for EE4 in order to provide a basis for a normal-coordinate analysis with subsequent calculations of vibrational amplitude quantities. Such supplementary information was needed to perform corrections for vibrational effects in the structure determination (shrinkage corrections) and to establish reasonable estimates and constraints for vibrational amplitude parameters (l-values) which could not be determined from the GED data alone.

In the absence of spectroscopic data shrinkage corrections were not performed in the previous GED-study of hexachloro-1,3-butadiene [3]. In course of the present investigation of EE4, it was also noted that applied assumptions regarding some of the l-values for HEX are, by comparison with calculated values for analogous parameters in EE4, rather unreasonable. A structural reinvestigation of HEX based on new GED data and spectroscopic data now available from the literature [9,10] was therefore included in the present investigation.

Finally, the minimum energy conformations and the torsional barriers are estimated for EE4 and HEX by molecular mechanics calculations, and the barriers to interconversion of the two enantiomeric non-planar forms (Fig. 1) are compared to literature data obtained by dynamic NMR.

EXPERIMENTAL

Samples

EE4 was prepared from *trans*-1,2-dichloroethene by oxidative coupling as described elsewhere [11]. The boiling points were 172–173 and 63–64°C at 760 and 16 torr, respectively. It was purified by fractional distillation in vacuo. Gas chromatographic analyses indicated a purity of at least 98.8%.

A commercial sample of HEX with a stated purity of about 99% was obtained from Aldrich-Chemie, West Germany. It was used without further purification.

Vibrational spectral data for EE4

Infrared spectra were recorded on a Perkin-Elmer model 225 spectrometer (4000–200 cm^{-1}) and with a Bruker IFS 114C FTIR instrument (600–20 cm^{-1}). Spectra were obtained of the neat liquid, of solutions, of the solid at

about 90 K and of the molecule isolated in nitrogen matrices at 13 K ($M/A \sim 1{:}1000$).

Raman spectra were obtained with a DILOR RTI 30 trippel monochromator interfaced to the data system of the FTIR instrument. The 488 nm line of a Coherent CRL 52G argon ion laser was used for excitation. The liquid sample was studied in a sealed glass tube and semi-quantitative polarization data were obtained.

Electron-diffraction data

Electron-diffraction diagrams of EE4 and HEX were recorded on Kodak Electron Image Plates in the Oslo Apparatus [12] at nozzle-tip temperatures of 363 and 373 K, respectively. Two different nozzle-to-plate distances were used giving a long- and a short-camera set of data for both compounds: EE4, five plates at 476.22 mm and five plates at 196.22 mm; and HEX, six plates at 484.80 mm and three plates at 204.94 mm.

The accelerating voltage was about 35 kV and the electron wavelengths as calibrated against diffraction patterns of gaseous benzene ($r_a = 139.75$ pm [13]), were for EE4 6.467; and for HEX 6.372 and 6.360 pm for the long- and short-camera data sets respectively. The estimated uncertainty in the s-scale is 0.1%.

The optical densities of the photographic plates were recorded as raster images on modified Mk III CS Joyce–Loebl microdensitometers at the Department of Theoretical Astrophysics and at the Department of Chemistry for EE4 and HEX respectively.

INTERPRETATION OF THE VIBRATIONAL SPECTRA

Infrared and Raman spectral data of HEX are reported in the literature [9] and they have been interpreted by overlay force-field calculations for 1,3-butadiene and several of its chlorine derivatives [10].

The infrared and Raman spectra of EE4 as a liquid at ambient temperatures are shown in Figs. 2 and 3, respectively and the important spectral data are collected in Table 1.

It is immediately clear from the data presented that EE4 cannot have C_{2h} symmetry (*anti* conformations, $\phi = 180°$) which requires mutual exclusion of the IR and Raman activities. Neither is C_{2v} symmetry (*syn* conformation, $\phi = 0°$) compatible with our data. Both of these symmetries are also prohibited by steric interactions as discussed previously. Hence EE4 can only have C_2 symmetry (see Fig. 1) according to which the normal modes of vibration divide into $\Gamma_v = 13a + 11b$, all of which are active both in the IR and Raman spectra, the $13a$ modes being Raman polarized. Unfortunately the vapour pressure of EE4 was too low to enable us to record the IR vapour-phase spectrum in a 10-

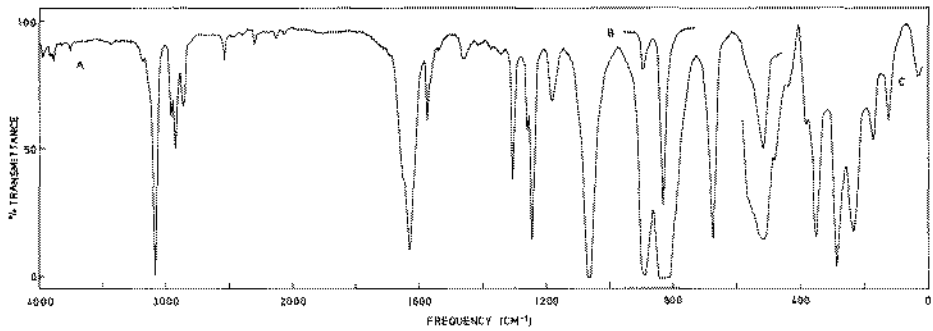

Fig. 2. Infrared spectra of *trans,trans*-1,2,3,4-tetrachloro-1,3-butadiene, in the liquid phase (A and B) and in benzene solution (C).

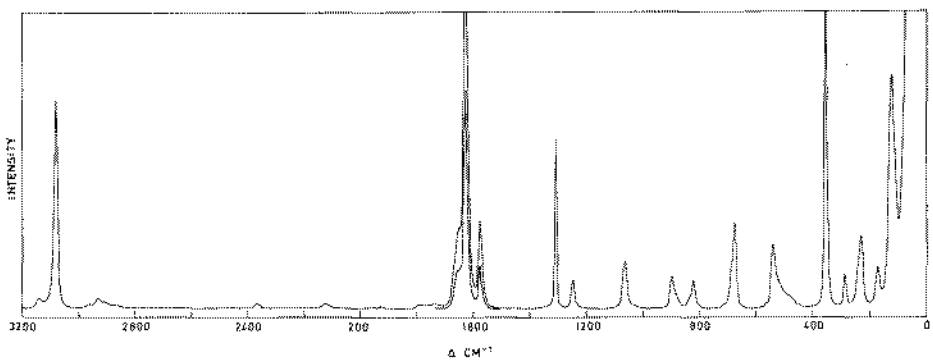

Fig. 3. Raman spectrum of *trans,trans*-1,2,3,4-tetrachloro-1,3-butadiene, in the liquid phase.

cm long cell. Consequently, the *a*- and *b*-modes were distinguished only by their polarization ratio in the Raman spectrum.

The majority of the fundamental modes are readily assigned on the basis of the polarization measurements alone (c.f. Table 1): $\nu_1 - \nu_4$ and $\nu_6 - \nu_9$ of species *a*; and ν_{15}, ν_{16}, ν_{18}, ν_{19} and $\nu_{22} - \nu_{24}$ of species *b*. The further interpretation of the data relies in part upon a normal coordinate analysis in which a standard valence force field was constructed by the overlay technique using a computer program VIBFIT and the data on *cis*- and *trans*-1-chloro-1,3-butadiene [14], *cis,cis*-, *trans,trans*- and *cis,trans*-1,4-dichloro-1,3-butadiene [15,16], 2-chloro-1,3-butadiene [10,17] and 2,3-dichloro-1,3-butadiene [10,18]. Thus $\nu_{10}(a)$, $\nu_{12}(a)$, $\nu_{17}(b)$ and $\nu_{20}(b)$ are assigned to weak shoulders in the Raman effect which have no polarization measurements. The band at 352 cm^{-1} splits into two components in the spectra of the crystalline phase and $\nu_5(a)$ and $\nu_{21}(b)$ are taken to be overlapping. Similarly $\nu_5(a)$, the C–H(bop) which is normally strong in the IR region, but weak in Raman, is taken to be overlapped by the $\nu_{18}(b)$ mode at 895 cm^{-1}. Both in the matrix spectra and in the spectra of the crystalline phase this band splits into two components. More uncertain is our

TABLE 1

Infrared and Raman spectral data for *E,E*-1,2,3,4-tetrachloro-1,3-butadiene (EE4)[a,b]

Infrared			Raman		Interpretation
N_2 matrix 13 K	Liquid/ solution[c]	Polycryst. solid 90 K	Liquid	Polycryst. solid 90 K	
		3090 w		3093 w,sh	
3100 m	3081 s	3080 s	3081 s,P	3082 vs	ν_1 *a*, ν_{14} *b*
	1652 w,sh	1658 vw	1655 w,P	1655 m-w	
		1642 w		1644 w	
1628 m	1628 m	1636 vw	1628 vs,P	1628 s	ν_2 *a*
		1624 w		1615 w	
1584 w	1576 w	1579 w	1577 m,D	1581 m	ν_{15} *b*
	1567 vw,sh		1569 w,sh	1566 w	
	1535 vw				
	1464 vw				
	1457 vw				
	1410 vw				
	1378 vw				
	1345 vw				
1312 w	1306 w	1307 w	1308 s,P	1307 s	ν_3 *a*
1264 w	1261 w	1264 vw			
1254 w	1245 m	1254 w	1246 m,D	1248 m	ν_{16} *b*
1250 w					
1190 vw	1182 w,br	1180 vw			
	1130 vw				
1077 vw		1088 vw			
1068 w		1069 w		1070 w	
1063 s	1062 s	1059 m	1064 m,P	1063 m	ν_4 *a*
		1049 vw			
		1046 vw			
1025 vw	~ 1025 w,sh	1025 vw	~ 1025 vw	1020 vw	ν_{17} *b*
			~ 950 vw		
	~ 930 vw,sh				
904 s		899 s		902 m	
	896 s		895 m,D		
898 m		895 s		~ 895 w,sh	ν_5 *a*, ν_{18} *b*
	~ 875 m,sh	885 w	~ 880 w,sh		
866 vw		866 w		868 w	
		838 vs			
840 vs	832 vs		832 w,D	835 w	ν_{19} *b*
		831 vs			
830 m	~ 815 m,sh	825 vs	820 m,P	821 m	ν_6 *a*
822 w					
	790 w,sh				
	765 w,sh				
	~ 720 vw,sh				

TABLE 1 (*continued*)

Infrared			Raman		Interpretation
N_2 matrix 13 K	Liquid/ solution[c]	Polycryst. solid 90 K	Liquid	Polycryst. solid 90 K	
678 w				692 vw	
671 m	674 s	670 s	674 m,P	671 s	$\nu_7\, a$
		664 w			
	632 vw				
	570 vw		570 vw,sh		
	545 vw	545 vw			
532 vw		540 vw	540 m,P	545 m	$\nu_8 a$
528 vw					
515 w	517 m	510 s	~ 515 w,sh	515 w	$\nu_{20}\, b$
512 w					
	481 vw,sh		~ 480 vw,sh	468 vw	
	379 vw	375 vw			
		363 vw			
		354 m		355 vs	
~ 350 vw	349 m		352 s,P		$\nu_9\, a$, $\nu_{21}\, b$
		350 m		350s,sh	
283 m	285 m	288 s	284 m,D	288 w	$\nu_{22}\, b$
238 vw		245 m	~ 240 w,sh	236 m	$\nu_{10}\, a$
	232m				
217 w		225 m	230 m,D	223 w	$\nu_{23}\, b$
	173 w	183 w	170 m,D?	182 w	$\nu_{11}\, a$
		135 m	122 s,D	138 s	$\nu_{24}\, b$
	123 w				
		123 vw	~ 110 m,sh	123 m	$\nu_{12}\, a$
				79 s	
		70 w		68 s	
		60 w		59 s	
				46 m	
				35 s	
	34 vw		~ 40 ?		$\nu_{13}\, a$

[a]Bands in the region 5000–3100 cm^{-1} and 3000–1700 cm^{-1} have been omitted.
[b]Abbreviations: s, strong; m, medium; w, weak; v, very; sh, shoulder; P, polarized; D, depolarized.
[c]Values 481 cm^{-1} and below are from a 10% solution in benzene.

assignment of $\nu_{11}(a)$ to the bands around 170 cm^{-1} which appears to be depolarized like all the other bands below 300 cm^{-1} in the Raman effect. However, all reasonable force fields predict an a-mode and not a b-mode at about 170 cm^{-1}. The low lying torsional mode about the central bond, $\nu_{13}(a)$, was tentatively assigned to an uncertain band at 40 cm^{-1}. In HEX the corresponding fundamental was 44 cm^{-1} as compared to a value of 30 cm^{-1} calculated from the overlay force field [10].

TABLE 2

A valence force field for *trans,trans*-1,2,3,4-tetrachloro-1,3-butadiene (EE4)[a]

Diagonal elements		*Interaction elements*	
Stretch (f_r)		*Stretch* ($f_{r,r}$)	
C=C	8.30	C=C/C-C	0.70
C-C	5.40	C=C/C-Cl	0.28
C2-Cl	3.52	C-C/C-Cl	0.28
C1-Cl	3.69		
C-H	5.16		
		Stretch/bend ($f_{r,\delta}$)	
		C=C/C=C-H	0.24
Bend (f_δ)		C-Cl/Cl-C-H	0.20
C=C-C	0.94	C-Cl/C=C-Cl	0.65
C1=C2-Cl	1.11	C-Cl/C-C-Cl	0.65
C3-C2-Cl	1.11	C=C/C=C-C	0.57
C2=C1-H	0.50	C-C/C=C-C	0.44
C2=C1-Cl	1.11	C=C/C=C-Cl	1.00
Cl-C1-H	0.40	C-C/C=C-Cl	
Bend out-of-plane (f_γ)			
Cl,H-C=C	0.29		
Cl,C-C=C	0.41		
Torsion (f_τ)			
C=C	0.11[b]		
C-C	0.12		

[a]The units are $f_r, f_{r,r}$: mdyn A^{-1} (100 aJ nm^{-2}); $f_\delta, f_\gamma, f_\tau$: mdyn Å rad^{-2} (aJ rad^{-2}); and $f_{r,\gamma}$ mdyn rad^{-1} (10 aJ nm^{-1} rad^{-1}). 1 aJ = 10^{18} J = 1 mdyn Å.
[b]Four contributions, i.e. totally f_τ (C=C) = 0.44 aJ rad^{-2}.

TABLE 3

Observed[a] and calculated[b] frequencies (cm^{-1}) for *trans,trans*-1,2,3,4-tetrachloro-1,3-butadiene (EE4)

Species	Obs.	Calc.	Species	Obs.	Calc.
a ν_1	3081	3080	*b* ν_{14}	3081	3081
ν_2	1628	1610	ν_{15}	1577	1581
ν_3	1308	1326	ν_{16}	1246	1247
ν_4	1064	1062	ν_{17}	1025	974
ν_5	895	903	ν_{18}	895	865
ν_6	820	812	ν_{19}	832	813
ν_7	674	765	ν_{20}	515	581
ν_8	540	583	ν_{21}	352	366
ν_9	352	367	ν_{22}	284	324
ν_{10}	240	230	ν_{23}	230	211
ν_{11}	170?	169	ν_{24}	122	117
ν_{12}	110	93			
ν_{13}	40?	30			

[a]Raman liquid values.
[b]From the overlay force field described in the text.

A suggested set of force constants for EE4 is given in Table 2. The assigned fundamentals are given in Table 3 together with calculated counterparts obtained from the normal coordinate analysis. In these calculations the adopted geometry of the molecule was consistent with the final structural results (i.e., *synclinal* conformation).

STRUCTURE ANALYSES

Reduction of the GED-data

The GED data were treated by standard data reduction methods [19] to yield the total electron-diffraction scattering intensities (actually, $s^4 I_{tot}(s)$). The blackness correction applied on the measured densities (D) was $1.0+0.03D+0.09D^2+0.03D^3$. The curves were then multiplied by a modification function [19], $s/|f'_C(s)||f'_{Cl}(s)|$. The scattering amplitudes, $|f'(s)|$, and phases, $\eta(s)$, were calculated using the partial-wave method [20] based upon analytical Hartree–Fock potentials [21] for the carbon and chlorine atoms, and the best electron density of bonded hydrogen for the hydrogen atom [22].

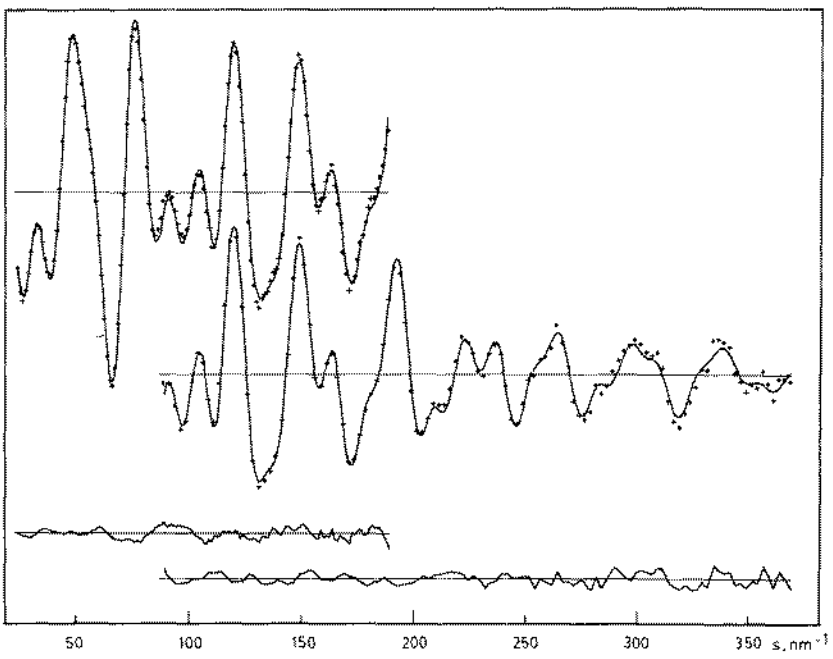

Fig. 4. Observed modified molecular intensities (+) for *trans,trans*-1,2,3,4-tetrachloro-1,3-butadiene (EE4) and calculated counterparts (full line) from the r_α-model in Table 5; and (below) the corresponding difference intensity curves.

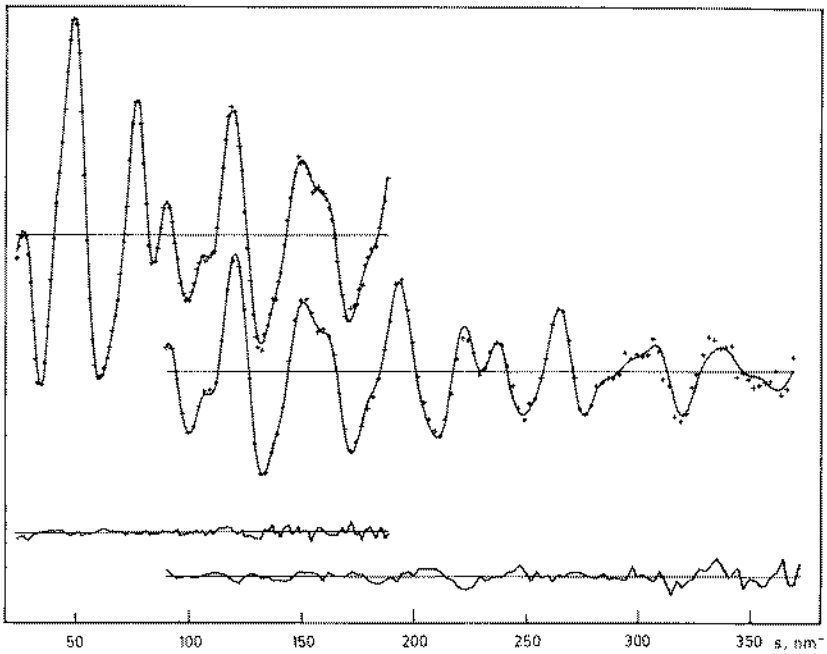

Fig. 5. Observed modified molecular intensities (+) for hexachloro-1,3-butadiene (HEX) and calculated counterparts (full line) from the r_α-model in Table 6; and (below) the corresponding difference intensity curves.

TABLE 4

Ranges and weighting of the electron-diffraction data in the structure refinement of *trans,trans*-1,2,3,4-tetrachloro-1,3-butadiene (EE4) and of hexachloro-1,3-butadiene (HEX)[a]

Camera height	Data range			Constants of the weighting scheme[b]					
	s_{min}	s_{max}	Δs	s_1	s_2	w_1	w_2	p_2	p_3
Long	25.0	190.0	1.25	50.0	190.0	0.0015	0.0	−0.64	0.146
Short	90.0	370.0	2.50	90.0	250.0	0.0	0.0001	−0.60	0.125

[a] s-values in nm^{-1}, and w-values in nm^2.
[b] See refs. 19 and 24 for meaning of the symbols. For diagonal weight matrices $p_2 = p_3 = 0$. Each data set was given equal weight.

An automatic background subtraction routine, analogous to that described by L. Hedberg [23], was applied to the modified total intensities to yield modified molecular intensity curves. For both compounds the resulting intensities for each camera distance were scaled and averaged. The final long- and short-camera experimental intensities upon which the structure analyses are based are shown in Figs. 4 and 5 for EE4 and HEX respectively. Diagonal weighting

of the data was used in the structure determinations which were carried out by the least-squares method. However, the standard deviations thus obtained (σ_{LS}) were augmented by a factor of two to account for correlation in the data as indicated by comparative refinements using diagonal and non-diagonal [24]

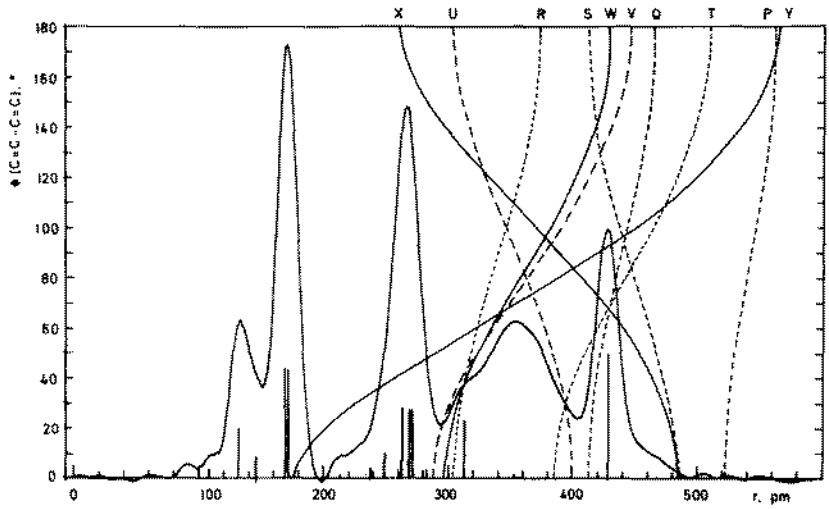

Fig. 6. Experimental radial distribution curve for *trans,trans*-1,2,3,4-tetrachloro-1,3-butadiene (EE4) and the interatomic distance distribution; the vertical bars and the P to Y (cf. Table 7) curves (distance as a function of the torsional angle, ϕ) represent torsion independent and torsion dependent interactions respectively.

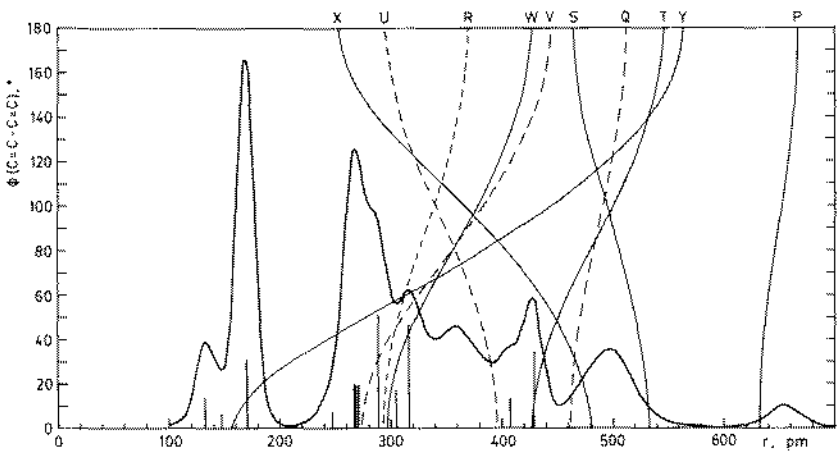

Fig. 7. Experimental radial distribution curve for hexachloro-1,3-butadiene (HEX) and the interatomic distance distribution; the vertical bars and the P to Y (cf. Table 8) curves (distance as a function of the torsional angle, ϕ) represent torsion independent and torsion dependent interactions respectively.

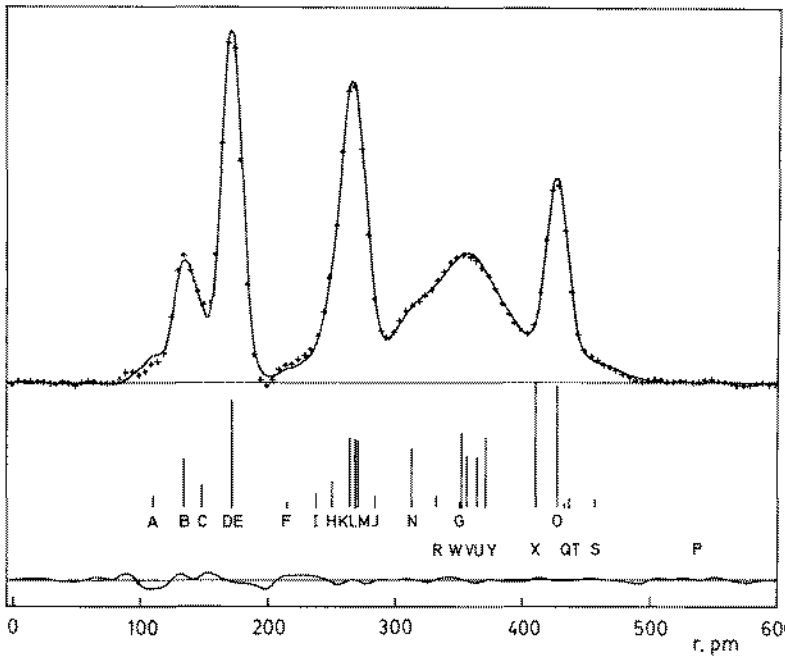

Fig. 8. Experimental (+) and theoretical (full line) radial distributions and the corresponding difference curve for *trans,trans*-1,2,3,4-tetrachloro-1,3-butadiene (EE4) calculated from the data in Fig. 4. The line diagram shows final interpretation of the curve (cf. Table 8).

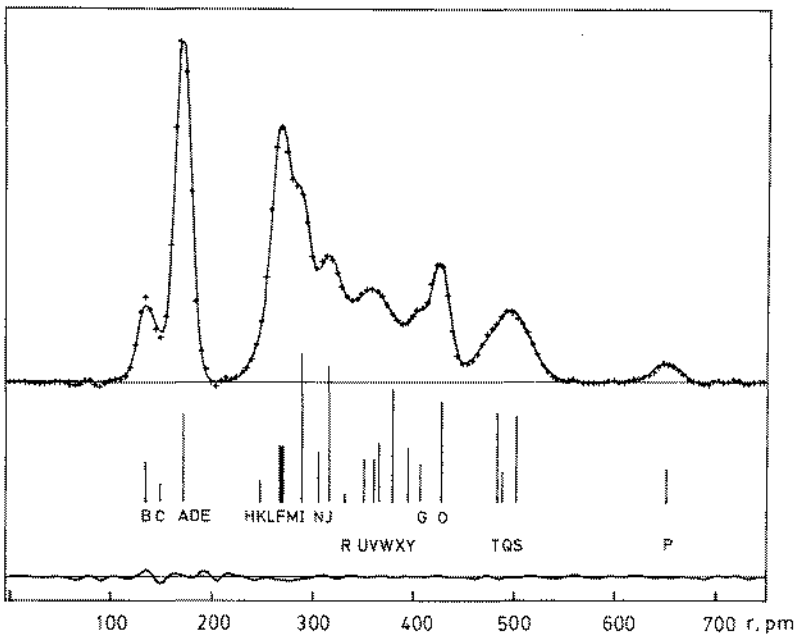

Fig. 9. Experimental (+) and theoretical (full line) radial distributions and the corresponding difference curve for hexachloro-1,3-butadiene (HEX) calculated from the data in Fig. 5. The line diagram shows final interpretation of the curve (cf. Table 9).

weighting. Data ranges and constants in the weighting schemes are specified in Table 4.

Corresponding long and short camera intensity data were also scaled and averaged in the overlap region to yield one continuous intensity curve for each of the two compounds. Fourier inversion of these data using a damping function $\exp(-bs^2)$ where $b=1.5\ 10^{-5}\ \mathrm{nm}^{-2}$, and pertinent theoretical intensity values for the unobserved inner region (i.e. $s<25.0\ \mathrm{nm}^{-1}$) gave experimental radial distribution curves, RD(r), for EE4 and for HEX as shown in Figs. 6 to 9.

Model descriptions

Perspective views of the EE4 and HEX molecules are shown in Fig. 10. Their geometries under C_2 symmetry are specified by ten independent parameters assuming planarity at each carbon atom. They are defined in Tables 5 and 6 for EE4 and HEX respectively. The twenty-five different interatomic interactions, which have each a dependent distance parameter (r_a) and an independent vibrational parameter (l), are listed in Table 7 for EE4 and in Table 8 for HEX. The supplementary vibrational amplitude quantities needed for the more comprehensive structural analysis were ultimately calculated at pertinent temperatures using a normal-coordinate computer program ASYM20 [25]: l, the r.m.s. vibrational amplitude; K, the perpendicular amplitude correction coefficients; and dR, the centrifugal stretching of the distances. Some of the calculated l-values were used as fixed parameter estimates or in establishing reasonable relations in grouped refinements of amplitude parameters. Non-zero anharmonicity constants, κ [19], for the bond distances were estimated from the diatomic approximation by $\kappa=1/6al^4$, where $a=20\ \mathrm{nm}^{-1}$ [26].

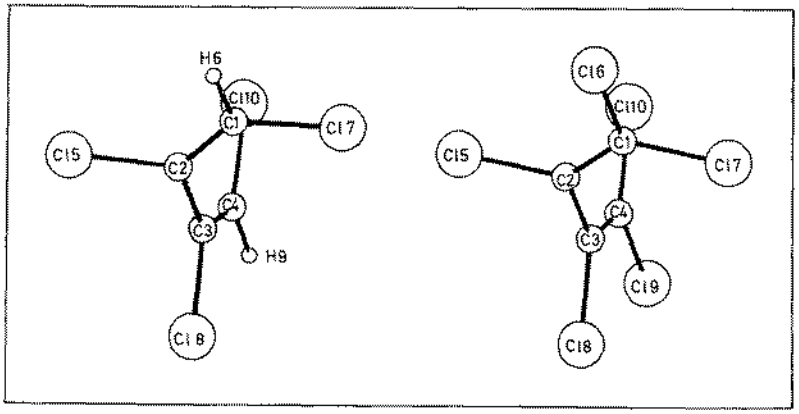

Fig. 10 Perspective views of the *synclinal* conformations of *trans,trans*-1,2,3,4-tetrachloro-1,3-butadiene (EE4), left and of hexachloro-1,3-butadiene (HEX), right with numbering of atoms.

TABLE 5

Results for the structural parameters of *trans,trans*-1,2,3,4-tetrachloro-1,3-butadiene (EE4) obtained by gas-phase electron diffraction (GED) and molecular mechanics calculations (MM). Distances (r) in pm and angles ($\angle, \phi, \delta$) in degrees[a]

	GED (r_α-model)[b]		GED (r_α'-model)[c]		MM
	$r_\alpha, \angle_\alpha$	$r_a = r_\alpha - D$	$r_\alpha', \angle_\alpha'$	$r_a = r_\alpha' - D$	$r_e, \angle_e$
r(C–H)	108.4 (-)	110.0(-)	108.4 (-)	109.9(-)	110.8
r(C=C)	133.6 (5)	134.3(5)	133.9 (5)	134.2(5)	134.6
r(C–C)	148.0 (8)	148.1(8)	147.7 (9)	147.8(9)	148.5
r(C1–Cl)	170.6 (3)	172.5(3)	171.8 (3)	172.4(3)	172.0
$\Delta = r$(C2–Cl) $-r$(C1–Cl)	0.62(-)	0 (-)	0.12(-)	0 (-)	−0.1
$\angle$ (C1=C2–C3)	125.7 (4)		125.6 (4)		124.8
$\angle$ (C3–C2–Cl)	115.6 (4)		115.2 (4)		114.8
$\angle$ (C2=C1–Cl)	122.4 (5)		122.8 (6)		121.4
$\angle$ (C2=C1–H)	124.0 (-)		124.0 (-)		121.4
ϕ(C=C–C=C)	76.6 (23)		77.8 (20)		85.6
δ(C=C–C=C)	-		16.3 (16)		-
R(lsq)[d]	7.81%		8.19%		

[a]Values in parentheses are estimated standard deviations (σ) accounting for data correlation and for the distances the uncertainty of the s-scale: $\sigma = \Sigma[(2\sigma_{LS})^2 + (0.001r)^2]^{1/2}$; (-) denotes unrefined quantities.

[b]The interatomic distances (r_a) and vibrational amplitude quantities are given in Table 7, and the corresponding correlation matrix and σ_{LS}-quantities in Table 9.

[c]The calculated l' and D' values are given in Table 7. The refined l-values were l' (D) = 4.9(2), l' (K) = 6.8(3), l' (N) = 15.4(16) and l' (0) = 6.5(3) pm; and the largest element of the correlation matrix $\rho(\phi,\delta) = +0.62$.

[d]R(lsq) = $100[\Sigma w_i \Delta_i^2 / \Sigma w_i I_i^2$ (obs)$]^{1/2}$; $\Delta_i = I_i$ (obs) $- I_i$ (calc).

A more important correction of vibrational effects is, however, the inclusion of shrinkage corrections. This could be performed by a r_α-model which specifies the geometries in terms of r_α-type parameters (Tables 5 and 6). The corresponding sets of geometrically consistent r_α interatomic distances were then converted to the geometrically inconsistent set of r_a counterparts which are required by the GED intensity expression [19] by the relation $r_a = r_\alpha - D$; $D = l^2/r - K - dR$ [27]. The magnitudes of the three terms showed that dR [28] should not be omitted in the computation of the conversion term.

The final molecular force fields for EE4 and HEX, established by the use of ASYM20 [25], reproduced the observed normal modes (EE4, Table 3; and HEX [10] which contains no force-field specification) to within deviations of less than 10 cm^{-1}. Various levels of goodness-of-fit and slight changes in the interpretation of the spectroscopic data appeared to be immaterial for the analyses of the GED data. However, the assignments of the low-lying torsional modes are uncertain (i.e. $\nu_{13}(a)$ for EE4) which in particular affects greatly

TABLE 6

Results for the structural parameters of hexachloro-1,3-butadiene (HEX) obtained by gas-phase electron diffraction (GED) and molecular mechanics calculations (MM). Distances (r) in pm and angles ($\angle$, ϕ, δ) in degrees[a]

	GED (r_α-model)[b]		GED (r_α'-model)[c]		MM
	r_α, $\angle_\alpha$	$r_a = r_\alpha - D$	r_α', $\angle_\alpha'$	$r_a = r_\alpha' - D$	r_e, $\angle_e$
r(C–Cl7)	169.5 (3)	171.6(3)	170.7 (3)	171.6(3)	172.3
$\Delta = r$(C2–Cl) − r(C1–Cl7)	0.51(-)	0 (-)	−0.04(-)	0 (-)	0.7
$\Delta = r$(C1–Cl6) − r(C1–Cl7)	0.75(-)	0 (-)	−0.51(-)	0 (-)	0 (-)
r(C=C)	133.3 (5)	134.1(5)	133.7 (5)	134.1(5)	135.3
r(C–C)	148.2 (9)	148.5(9)	148.2 (9)	148.5(9)	148.0
$\angle$(C1=C2–C3)	122.6 (4)		122.4 (4)		122.3
$\angle$(C3–C2–Cl)	115.8 (4)		115.8 (4)		113.8
VCCl[d]	122.50(10)		122.59(10)		122.0
ΔCCl[d]	−0.9 (6)		−0.5 (6)		−3.0
ϕ(C=C–C=C)	89 (3)		83.5 (19)		84.9
δ(C=C–C=C)	-		12.0 (14)		-
R(lsq)[e]	6.53%		6.78%		-

[a] See corresponding note in Table 5.

[b] The interatomic distances (r_α) and vibrational amplitude quantities are given in Table 8, and the corresponding correlation matrix and σ_{LS}-quantities in Table 10.

[c] The calculated l' and D' values are given in Table 8. The refined l-values were l' (A) = 5.19(17), l'(D) = 4.75(A), l'(E) = 5.11(A), l'(F) = 6.63(20), l'(G) = 7.1(10), l'(I) = 6.8(3), l'(J) = 11.7(5), l'(K) = 6.22(F), l'(L) = 4.46(F), l'(M) = 7.12(F), l'(N) = 13.4(J), l'(O) = 6.9(3).

[d] $\angle$(C2=C1–C16) = VCCl − ΔCCl/2; $\angle$(C2=C1–C17) = VCCl + ΔCCl/2.

[e] See footnote d in Table 5.

the l-values associated with the torsion-sensitive distances and the shrinkage correction. According to the potential energy distributions in the normal coordinate calculations this normal mode (ν_τ) is fairly pure for both EE4 and HEX. Consequently the corresponding torsional force constant, f_τ, could be varied without great changes in the calculated values for the remaining fundamental frequencies. Different sets of l- and D-values thus obtained were used in the GED structure analyses in attempts to gain information about f_τ and thereby ν_τ from the GED data. Some relevant sets of f_τ (in aJ rad^{-2}) and ν_τ (in cm^{-1}) values are: for EE4, 0.06/25; 0.115/32 and 0.187/40; and for HEX 0.12/32 and 0.25/44. The l- and D-values calculated using $f_\tau = 0.115$ aJ rad^{-2} for EE4 and $f_\tau = 0.12$ aJ rad^{-2} for HEX are given in Table 7 and 8 respectively, and the f_τ dependencies of the l-values associated with the torsion-sensitive distances are exemplified by the values given in footnote c to these Tables.

The torsion about the central C–C bond may also be investigated by using a dynamic model which separates this large amplitude motion from the rest of the molecular dynamics. This model, hereafter referred to as the r_α'-model

TABLE 7

Distances (r_a) and amplitudes (l) for the interatomic interactions in *trans,trans*-1,2,3,4-tetrachloro-1,3-butadiene (EE4) corresponding to the results of the r_α-model (Table 5); and the calculated (see text) vibrational amplitude quantities l and D (r_α-model) and the corresponding framework values l' and D' (r_α'-model). All quantities in pm

Interactions[a]	GED results[b]		Calculated quantities[c]			
	r_a	l	l	D	l'	D'
A (2): C1–H	110.0		7.71	−1.57	7.71	−1.50
B (2): C1=C2	134.3(5)		4.46	−0.69	4.46	−0.31
C (1): C2–C3	148.1(8)		4.99	−0.15	4.99	−0.14
D (2): C1–Cl	172.5(3)	5.0(2)	5.17	−1.88	5.17	−0.65
E (2): C2–Cl	172.5(3)	5.1(D)	5.30	−1.26	5.30	−0.53
F (2): C2··H6	215.1(5)		10.14	−1.11	10.14	−0.92
G (2): C3··H6	351.2(12)		9.96	−0.82	9.96	−0.73
H (2): C1··C3	251.0(11)		6.16	−0.41	6.16	−0.25
I (2): H6··C17	237.6(9)		11.61	−1.73	11.61	−0.74
J (2): H6··C15	284.3(13)		15.10	−1.20	15.10	−0.10
K (2): C1··C15	264.6(9)	6.8(3)	7.01	−1.57	7.01	−0.29
L (2): C2··C17	269.3(8)	6.4(K)	6.68	−2.11	6.68	−0.36
M (2): C3··C15	271.1(9)	7.2(K)	7.46	−0.80	7.46	−0.26
N (2): C3··C17	313.7(18)	13.5(13)	11.31	−1.49	11.31	−0.11
O (2): C15··C17	428.1(7)	6.5(2)	7.17	−2.70	7.17	−0.16
P (1): H6··H9	537.7(20)		11.61	−0.98	13.85	−0.81
Q (2): C1··H9	433.6(20)		12.76	−0.79	11.69	−0.58
R (1): C1··C4	332.6(21)		10.67	−0.47	8.19	−0.23
S (2): H6··Cl8	457.5(22)		15.71	−0.34	14.12	−0.31
T (2): H6··Cl10	437(4)		23.79	−0.90	19.54	−0.09
U (2): C1··Cl8	365(3)	19(6)	13.32	−0.01	10.00	−0.12
V (2): C1··Cl10	357(4)	22.4(17)	22.12	−0.66	14.17	0.01
W (1): Cl5··Cl8	353(3)	18.2(V)	17.87	−0.55	12.24	0.10
X (2): Cl5··Cl10	411(5)	35(5)	25.67	0.98	15.43	0.03
Y (1): Cl7··Cl10	371(8)	51(U)	45.00	3.18	14.43	0.47

[a]The letters A to Y identify the distances in the RD-curves; values in parentheses are the distance multiplicities (C_2-symmetry). See Fig. 10 for numbering of atoms.

[b]Numbers in parentheses are estimated standard deviations (see comment a in Table 5). Letters in parentheses for the l-values identify tied l-value groups; omitted l-values signify that the calculated values have been used.

[c]The torsional force constant was $f_\tau = 0.115$ aJ rad^{-2} ($\nu_\tau = 32$ cm^{-1}). For $f_\tau = 0.06$ aJ rad^{-2} ($\nu_\tau = 25$ cm^{-1}) the P to Y l-values were: 14.9, 13.7, 12.7, 17.2, 26.8, 16.1, 27.1, 22.4, 32.2 and 58.2 pm.

requires framework vibrational amplitude parameters. These l'- and D'-values are included in Tables 7 and 8 and they were obtained by omitting the contributions from the ν_τ (C–C) modes in the normal-coordinate calculations. The r.m.s. torsional angle amplitude, δ, was then used in the specifications of the

TABLE 8

Distances (r_a) and amplitudes (l) for the interatomic interactions in hexachloro-1,3-butadiene (HEX) corresponding to the results of the r_α-model and the calculated (see text) vibrational amplitude quantities: l and D (r_α'-model) and the corresponding framework values l' and D' (r_α-model). All quantities in pm

Interactions[a]	GED results[b]		Calculated quantities[c]			
	r_a	l	l	D	l'	D'
A (2): C1–Cl6	171.6 (3)	5.22 (16)	5.56	−1.35	5.56	−1.33
B (2): C1=C2	134.1 (5)	–	4.67	−0.84	4.67	−0.42
C (1): C2–C3	148.5 (9)	–	5.02	−0.32	5.02	−0.29
D (2): C1–Cl7	171.6 (3)	4.76 (A)	5.10	−2.10	4.73	−0.82
E (2): C2–Cl5	171.6 (3)	5.14 (A)	5.48	−1.59	5.11	−0.86
F (2): C2···Cl6	268.6 (7)	6.66 (19)	7.12	−1.38	6.63	−1.16
G (2): C3···Cl6	407.2 (7)	6.5 (9)	6.85	−0.87	7.06	−0.75
H (2): C1···C3	247.4 (11)	–	7.13	−0.44	7.13	−0.29
I (2): Cl6···Cl7	288.8 (6)	6.8 (3)	7.00	−2.31	6.78	−1.50
J (2): Cl6···Cl5	316.6 (11)	11.4 (6)	11.99	−1.56	11.70	−0.50
K (2): C1···Cl5	267.1 (6)	6.26 (F)	6.72	−1.76	6.22	−0.47
L (2): C2···Cl7	267.9 (7)	6.49 (F)	6.95	−2.42	6.46	−0.58
M (2): C3···Cl5	270.8 (10)	7.15 (F)	7.61	−1.12	7.12	−0.50
N (2): C3···Cl7	305.1 (20)	13.1 (J)	13.72	−1.43	13.43	−0.05
O (2): Cl5···Cl7	428.1 (8)	6.9 (3)	7.21	−3.01	6.93	−0.42
P (1): Cl6···Cl9	652.1 (14)	13.2 (18)	12.93	−0.30	11.91	−0.23
Q (2): C1···Cl9	489 (2)	17 (3)	13.33	−0.46	11.82	−0.37
R (1): C1···C4	332 (3)	–	13.16	−0.21	10.26	−0.16
S (2): Cl6···Cl8	503 (3)	16.7 (12)	14.47	−0.32	12.43	−0.16
T (2): Cl6···Cl10	483 (4)	32 (Q)	28.81	0.02	24.17	0.37
U (2): C1···Cl8	351 (3)	13.4 (13)	14.29	−0.16	10.83	−0.20
V (2): C1···Cl10	360 (5)	24.8 (U)	25.70	−0.04	16.96	0.09
W (1): Cl5···Cl8	366 (5)	18.8 (U)	19.73	−0.44	15.63	0.33
X (2): Cl5···Cl10	379 (8)	33.0 (4)	29.21	1.25	20.67	0.45
Y (1): Cl7···Cl10	395 (11)	51.1 (X)	47.35	4.00	14.71	−0.58

[a,b] See corresponding notes in Table 7.

[c] The torsional force constant was $f_\tau = 0.12$ aJ rad^{-2} ($\nu_\tau = 32$ cm^{-1}). For $f_\tau = 0.25$ aJ rad^{-2} ($\nu_\tau = 44$ cm^{-1}) the P to Y l-values were: 12.6, 12.8, 11.9, 13.6, 27.3, 12.4, 22.4, 16.9, 25.0 and 37.8 pm.

EE4 and HEX geometries (Tables 5 and 6), and the molecules were treated as mixtures of nine pseudoconformers [29]. The pseudoconformers have torsional angles $\phi_i = \phi_0 \pm \Delta\phi_i$ where $\phi_i = 0$, $1/2\delta$, δ, $3/2\delta$, and 2δ, and they were weighted according to a Gaussian potential function. Instead of determination of the l-values associated with the torsion-dependent distances the δ-parameter was refined and it is directly related to the torsional force constant by $f_\tau = RT\delta^{-2}$ [29].

The chosen dynamic model (r_α') is based upon a harmonic torsional poten-

tial as is the r_α-model. However, it should give a better treatment of the shrinkage corrections as the nine pseudoconformers give an overall asymmetric distance distribution for torsion-sensitive interatomic interactions. Model inspections (Fig. 1) would predict that the barriers of rotation are much higher in *syn* than in *anti* forms. The torsional potential is consequently asymmetric but investigations of its exact shape based on the GED data were not feasible.

It should also be noted that the geometrical parameters employed by the two models r_α and r_α' do not represent the same physical quantity. This is also seen from the fact that corresponding D and D' conversion terms (cf. Tables 7 and 8) differ for all interatomic interactions including bond distances. The r_a counterparts to the r_α and r_α' bond lengths are therefore included in Tables 5 and 6. In addition, corresponding D'-values will vary from conformer to conformer also for the geometrically independent distances. A rigorous treatment of the framework shrinkage correction in the r_α'-model therefore requires that all interactions are repeated for the nine pseudoconformers. However, in the present work only torsion-dependent interactions were repeated and D'-values for $\phi = \phi_0$ were used for the remaining distances.

Geometrical constraints

For both molecules attempts were made throughout the analyses to determine all ten geometrical variables, but ultimately constraints or assumptions were required.

For EE4 the r(C–H) and $\angle$C–C–H parameters tended to attain slightly unreasonable values (for example, $r_\alpha = 106(2)$ pm and $\angle_\alpha = 130(3)°$). They were therefore constrained to values (Table 5) which are close to those of the corresponding parameters in *cis,cis*-1,4-dichloro-1,3-butadiene [2] and *trans*-1,2-dichloroethene [30–32].

Attempts at unambiguous determination of the relative magnitudes of the two types of C–Cl bond distances in EE4 failed. Although the difference parameter in most cases was slightly positive (i.e., r(C2–Cl) > r(C1–Cl)) it was not consistently so and never significantly different from zero. A constraint so as to give r_a(C1–Cl) = r_a(C2–Cl) for both the r_α and r_α' model was therefore ultimately introduced (Table 5). Similarly we could learn nothing about the relative lengths of the three types of C–Cl bonds in HEX and their r_a-values were assumed to be equal, as they were in the previous study [3]. The constraint that $\angle$C2=C1–Cl6 = $\angle$C2=C1–Cl7 (see Fig. 10 for numbering of the atoms) of the previous study was relaxed by introduction of a Δ(C2=C1–Cl) parameter (Table 6). Throughout the analysis both negative and positive start values for this Δ-parameter were used in order to avoid ambiguous results.

Interpretation of the RD-curves

Interpretations of the RD-curves are shown in Figs. 6 and 7. The interatomic distances that are invariant to the torsional angle parameter (ϕ) are represented by vertical bars and they account for all important features of the RD-curves to about $r = 330$ pm. The lengths of the remaining interatomic interactions are shown as a function of ϕ. Ruling out $r(\mathrm{Cl}\cdots\mathrm{Cl}) < 330$ pm it is seen that the molecules must take nearly perpendicular conformations with allowed ϕ-values in the 70–110° range. It should be noted that the van der Waals Cl···Cl distance is about 360 pm, but that closer interactions have been observed, for example, about 320 pm in 2,3-dichloro-1,3-butadiene [1] and *cis,cis*-1,4-dichloro-1,3-butadiene [2], and 346 pm in 2,2′-dichloro-biphenyl [33].

The $r(\phi)$ curves demonstrate that there are complex interchanges in the relative magnitudes of the distances for ϕ in the 70–110° range. The great variation in the lengths of several interactions are of course accompanied by large amplitudes of vibration associated with these distances as is also shown by the calculated l-values (Tables 7 and 8). The identifications of the various contributions to the RD(r) curve beyond 330 pm, i.e. determinations of the conformational angles. are therefore not straightforward. Both *synclinal* ($\phi < 90°$) and *anticlinal* ($\phi > 90°$) conformations were refined to ensure that unique determinations of ϕ were achieved. Vibrational amplitude quantities were then as calculated for geometries with appropriate ϕ-values.

For EE4 two minima were located, but a *synclinal* ($\phi = 75°$) conformation was invariably favoured over an *anticlinal* one ($\phi = 102°$) as seen from typical least-squares agreement factors of $R = 9.6\%$ and $R = 13.1\%$ respectively. A refinement where both conformers contributed gave minimum ($R = 9.1\%$) for a 72 to 28% mixture of the two forms which had $\phi_1 = 74°$ and $\phi_2 = 101°$. However no two-conformer minimum was obtained for HEX, and the *anticlinal* form ($\phi(\mathrm{start}) = 105°$) refined to a *synclinal* form.

Final refinements and results

The favoured *synclinal* forms of the r_α-models had $\phi = 75.0(10)°$ ($R(\mathrm{lsq}) = 9.6\%$) for EE4 and $\phi = 83.6(12)°$ ($R(\mathrm{lsq}) = 7.30\%$) for HEX when l- and D-values were as calculated from the established force fields using $f_\tau = 0.115$ aJ rad^{-2} for EE4 and $f_\tau = 0.12$ aJ rad^{-2} for HEX (Tables 7 and 8).

The determinations of bond distances and angles proved invariant to the choice of f_τ-values (in the range 0.06 to 0.25 aJ rad^{-2}) in the calculations of amplitudes and correction terms used in the structure refinement procedure, and to actual refinements of amplitude parameters (l and δ). The results presented in Tables 5 and 6 for these geometrical parameters are thus representative for all our refinements. Also the torsional angles were insensitive to refinements of l-values associated with torsion independent distances. Such

refinements improved the least-squares fit to $R=8.6\%$ for EE4 and $R=6.8\%$ for HEX, and the agreement between refined and calculated l-values was best for the latter molecule (Tables 7 and 8).

Refined l-values for torsion-sensitive distances (P to Y) are for EE4 larger than the calculated counterparts which correspond to $f_\tau=0.115$ aJ rad^{-2} and $\nu_\tau=32$ cm^{-1}. However, there are closer agreements between the two sets of l-values for HEX ($f_\tau=0.12$ aJ rad^{-2}, $\nu_\tau=32$ cm^{-1}) suggesting differences in the torsional force constants for these two molecules. This was corroborated by the determinations of the δ-parameters of the r_α'-models: the refined δ-value of 16.3° for EE4 corresponds to $f_\tau=0.06$ aJ rad^{-2} and $\nu_\tau=25$ cm^{-1} whereas the obtained $\delta=12.0°$ for HEX is consistent with the applied force constant of 0.12 aJ rad^{-2}.

Vibrational amplitude quantities obtained from f_τ-values corresponding to the possible ν_τ-assignments of 40 cm^{-1} ($f_\tau=0.187$ aJ rad^{-2}) and 44 cm^{-1} ($f_\tau=0.25$ aJ rad^{-2}) for EE4 and HEX were also used. This gave poorer fit to the data, even worse disagreements between calculated and refined counterparts for EE4 and such discrepancies were now also observed for HEX. For EE4 the refined l(U) to l(Y) values are in good agreement with those calculated using $f_\tau=0.06$ aJ rad^{-2} (footnote c, Table 7). Refinements based on such vibrational amplitude quantities for the assumed l-values and the D-values gave consistent results with respect to the refined and calculated l-values. However, for the most extensive refinements there was no improved fit to the data, and the geometrical parameter values were as presented for the r_α-model in Table 5.

A positive correlation between the torsional angle (ϕ) and its rms amplitude (δ) is observed for both molecules. The results of the most extensive refinements of the r_α-model were consistent with those of the r_α'-model for EE4. In contrast, the torsional angle in HEX was found to be 89(3) and 83.5(19)° by the r_α and r_α'-models respectively. The latter value is in agreement with that of the r_α-model with no refinement of the l-values. The correlations between ϕ and the individual l-value groups for torsion sensitive distances are shown in Tables 9 and 10. The r_α-models give a slightly better fit to the data, but this was achieved by more variables than the r_α'-models which determine one δ-parameter instead of several l-parameters for torsion-sensitive distances.

We have chosen to discuss the structural results in terms of those obtained by the most flexible r_α-model. The corresponding r_a interatomic distances and the refined l-values are presented in Tables 7 and 8 respectively for EE4 and HEX.

The good fits to the data demonstrated by the R(lsq)-values obtained, are also reflected by the difference intensity and difference RD-curves shown in Figs. 4 and 5 and in Figs. 8 and 9, respectively.

TABLE 9

Least-square standard deviations (σ_{LS}) and correlation matrix ($100\rho_{ij}$) for EE4 corresponding to the results of the r_α-model (Tables 5 and 7)

Parameter	σ_{LS}[a]	$100\rho_{ij}$															
r(C=C)	0.16	100															
r(C–C)	0.3	9	100														
r(C–Cl)	0.05	−13	19	100													
∠C1=C2–C3	0.2	22	12	19	100												
∠C3–C2–Cl	0.2	−12	−42	7	−32	100											
∠C2–C1–Cl	0.2	−48	−45	−22	27	32	100										
ϕ(C=C–C=C)	1.2	−14	−13	−13	−11	2	13	100									
l(D)	0.10	−18	−18	−6	−25	19	10	19	100								
l(K)	0.13	16	12	−20	−11	−48	−31	16	32	100							
l(N)	0.7	−7	−16	0	−15	2	−7	−33	−2	−13	100						
l(O)	0.12	−8	−1	−3	−12	4	0	−3	40	25	1	100					
l(U)	2.9	−10	−4	−1	−11	24	12	83	21	4	−43	−1	100				
l(V)	0.8	2	−6	−7	−16	−15	−21	−32	−3	8	55	3	−57	100			
l(X)	2.5	−8	−8	−4	−21	26	0	58	21	4	−14	1	62	−3	100		
S(1)	0.7	−17	−18	−9	−36	20	2	24	62	37	−3	37	26	4	33	100	
S(2)	1.3	−10	−2	−5	−19	9	1	15	72	41	−2	47	19	−6	17	51	100

[a]Distances and amplitudes in pm, angles in degrees; S are the scale factors for the two data sets: $S(1) = 76.3$ and $S(2) = 76.3$.

TABLE 10

Least-square standard derivations (σ_{LS}) and correlation matrix ($100\rho_{ij}$) for HEX corresponding to the results of the r_α-model (Tables 6 and 8)

Parameter	σ_{LS}[a]	$100\rho_{ij}$																				
r(C–Cl)	0.04	−100																				
r(C=C)	0.17	−35	100																			
r(C–C)	0.4	8	−30	100																		
∠C1=C2–C3	0.2	10	39	−12	100																	
∠C3–C2–Cl	0.2	0	−18	−29	−73	100																
VCCl	0.05	37	−41	−15	41	−10	100															
ΔCCl	0.3	−8	−8	37	39	−57	35	100														
ϕ(C=C–C=C)	1.7	−3	−13	3	−33	36	−12	−20	100													
l(A)	0.08	0	−8	−16	−11	11	0	−10	14	100												
l(F)	0.10	−10	11	−14	6	−18	−12	0	0	43	100											
l(G)	0.5	1	9	0	20	−22	5	17	−38	−2	2	100										
l(I)	0.13	1	−12	−6	−28	18	−14	−28	−1	30	51	0	100									
l(J)	0.3	6	4	2	56	−39	49	53	−51	−9	−2	26	0	100								
l(O)	0.16	−1	−1	−4	2	−5	0	3	−6	24	17	46	5	2	100							
l(P)	0.9	0	0	0	−1	0	0	0	2	4	3	0	1	−2	2	100						
l(Q)	1.5	−11	−13	−11	−30	25	−13	−17	76	20	10	−28	4	−45	−1	3	100					
l(S)	0.6	4	14	12	22	−18	0	11	15	1	3	0	−9	3	1	1	−4	100				
l(U)	0.7	0	14	0	34	−30	13	26	−74	−13	0	28	−1	51	1	−1	−61	−5	100			
l(X)	0.18	1	−7	0	0	22	21	5	51	0	−15	−14	−14	−2	0	0	30	8	−41	100		
S(1)	0.07	−3	−4	−24	−21	14	−18	−22	18	59	41	−5	26	−25	19	5	28	2	−18	−10	100	
S(2)	0.15	−2	−6	−5	−6	3	−1	−2	10	74	49	1	33	−1	27	4	15	3	−8	0	45	100

[a]See note in Table 9. $S(1) = 9.90$ and $S(2) = 9.44$.

MOLECULAR MECHANICS CALCULATIONS

It has been concluded [34] that simple molecular mechanics (MM) calculations reproduce simultaneously all trends in conformational energies, barrier heights and structural parameters for halogenated propenes, 1,3-butadienes and biphenyls and that the torsional force constants can also be estimated. We have carried out such calculations for both title compounds although HEX was one of the molecules included in the MM study mentioned [34]. No attempts were made to optimize the potential parameters which were values from the literature [34,35] except for the missing force constant (k) and reference value (θ_0) for the H–C(sp^2)–Cl angle which were taken to be $k=0.33$ aJ rad^{-2} [14,16] and $\theta_0=118°$. After a first set of calculations it was found [36] that the parameters in the Morse potential for the C(sp^2)$\cdots$Cl interaction ($R_o=260$ pm and $R_m=313$ pm) were unreliable, as they appeared to be based in part on incorrect experimental evidence, and instead $R_o=300$ pm and $R_m=353$ pm were recommended. These new values, which are also as obtained in parameterization based on fourteen halogenated propenes and butenes [37], were used in a new set of calculations. The new results were similar to the previous ones except that the torsional barriers and force constants were now somewhat lower, and we have chosen to report these latter results. Furthermore, no essential differences were obtained in calculations without and with excess charges estimated by the Sanderson method as described elsewhere [34], and the results of the former are reported in this paper.

The energies were calculated for fixed values of ϕ(C=C–C=C) in the 0° (*syn*) to 180° (*anti*) range with increments of 10°. In each case the remaining structural parameters were optimized and the resulting torsional potential curves (E) have energy minima at 80–90° as shown in Fig. 11. Minimum-

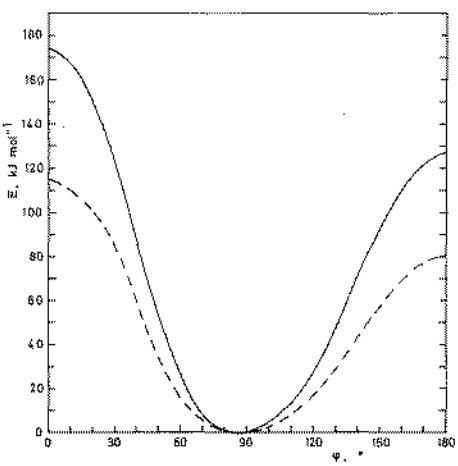

Fig. 11. Torsional potential curves (E) for *trans,trans*-1,2,3,4-tetrachloro-1,3-butadiene (EE4) (broken line) and of hexachloro-1,3-butadiene (HEX) (full line) obtained by molecular mechanics calculations.

energy structures were obtained by optimizing also the torsional angle, and the structural results are included in Tables 5 and 6 for EE4 and HEX, respectively. The corresponding torsional force constants were $f_\tau = 0.176$ aJ rad^{-2} for EE4, and $f_\tau = 0.293$ aJ rad^{-2} for HEX.

As also discussed subsequently it appears that these MM-calculations corroborate the experimental findings for these two nonplanar 1,3-butadienes satisfactorily for which the Cl···Cl interactions are probably the dominating energy terms. However, it should be noted that the predictions seem to be dubious for chloro derivatives which are in prevailing planar *anti* conformations [38]. In fact the results given in the original paper for 1,3-butadiene and 2,3-dichloro-1,3-butadiene [34] are not reproduced in our calculations when using the recommended set of parameter values.

DISCUSSION

It is shown by GED that EE4 and HEX both have non-planar, nearly perpendicular conformations. Furthermore, *synclinal* forms ($\phi < 90°$) appear to be favoured over *anticlinal* ones ($\phi > 90°$), most clearly so for EE4 which has $\phi = 76.6(3)°$. For HEX the preference of *syn* over *anti* is slightly ambiguous as the torsional angle in all refinements is closer to 90°, typical values being 83(2) to 89(3)°. The in effect perpendicular form, $\phi = 89(3)°$, was obtained in the most flexible refinement which shows that the determination of ϕ depends also on the relative magnitudes of some l-values. In conclusion, HEX is found to be more closely perpendicular than suggested by a previous study [3] which gave $\phi = 78(1)°$ using unrealistic assumptions for vibrational amplitude quantities. The MM calculations which gave reasonable results for bond distances and angles (see Table 5) supported the *synclinal* conformations, and suggested torsional angles were 84 to 86° for both molecules. The suggestion, based on the GED data, that EE4 has a wider torsional potential than HEX is corroborated by the MM results as seen from Fig. 11. The calculated torsional force constants for the two molecules also reflect this difference in vibrational properties as f_τ for EE4 is smaller than for HEX. This result was also obtained from analyses of the GED data, but the absolute values were much lower. The torsional frequencies suggested by the two methods are ν_τ (EE4) = 43 cm^{-1} and ν_τ (HEX) = 50 cm^{-1} by MM, and ν_τ (EE4) = 25 cm^{-1} and ν_τ (HEX) = 32 cm^{-1} by GED. Both determinations are rather uncertain and better vibrational spectroscopic data in the difficult low-frequency region are needed to settle this experimentally.

The two enantiomeric *synclinal* forms of EE4 and HEX (Fig. 1) interconvert by partial rotation about the central single bond via the planar *anti* forms. The MM results presented in Fig. 11 also demonstrate that planar *anti* is lower in energy than planar *syn* and according to these calculations the interconversion barrier is lowest for EE4: $E(anti) = 80.5$ kJ mol^{-1} as compared to

$E(anti) = 127.0$ kJ mol^{-1} for HEX. No experimental data exist for the barrier to enantiomerization in EE4 and HEX. However, from increments obtained by ^{1}H NMR studies of substituted (*E,E*)-tetrachloro-1,3-butadienes [7] the barriers can be estimated to 37 ± 2 and 67 ± 3 kJ mol^{-1} for EE4 and HEX, respectively. Thus the MM calculation reproduces the relative magnitudes of these two experimentally deduced barriers, but the absolute values are too high. The increased barrier in HEX may be ascribed to a buttressing effect of the "outer" terminal chlorine atoms (*trans* to C2–C3) [8]. Their non-bonding interactions with the inner chlorine atoms within each moiety of the molecule (i.e. Cl6 with Cl5 and Cl7 in Fig. 10) result in a greater rigidity. Therefore, the valence angle deformation necessary to reduce 1,3 interactions in the coplanar transition state is hindered, resulting in considerably higher barriers for HEX compared to EE4. In this context it is interesting to note that, according to the MM results, HEX also suffers more pronounced C–C and C=C bond elongation in the planar *anti* form which has C1=C2–C3, C2=C1–Cl (*cis*) and C2–C3–Cl angles of 130.9, 128.8, and 116.2° for EE4, and 129.9, 127.5 and 114.5° for HEX.

The valence angles and bond distances obtained for EE4 and HEX are compared with structural data for some analogous molecules in Table 11. The C=C–C angles in the listed chloro-1,3-butadienes may be considered in two categories according to their magnitudes relative to the corresponding angle in 1,3-butadiene itself, and the slightly compressed angles are found in molecules that have an "outer" terminal chlorine atom (*trans* to C2–C3). The C3–C2–Cl angles are similar in EE4, HEX, ZZ4 and D23 and r(C–Cl) and $\angle$(C2=C1–Cl) values for EE4 and HEX are in the range of values observed in other chlorinated 1,3-butadienes and in chloro derivatives of ethene. The C=C bonds in the twisted butadienes (EE4 and HEX) are similar in length to those found in the coplanar *anti* butadienes which are believed to be stabilized by conjugation effects. All these r(C=C) values are also in the range observed for the lengths of the localized C=C bonds in ethene and its derivatives. There are also only small variations in the length of the central C–C bond in the series of 1,3-butadienes and even in the nearly perpendicular molecules it is much shorter than the C–C bond in saturated hydrocarbons which for example is 153.3(2) pm in ethane [43] and 153.1(3) pm [44] in 1,2-dichloroethane. Excepting the values for ZZ4 from the comparison the results could indicate that slightly longer C–C bonds tend to occur in the non-planar molecules, but the effect is small and could for example be related to substitution effects or larger steric repulsions which are responsible for the non-planarity of the molecules. The central C–C bond is also found to be short in other non-planar 1,3-butadienes; for example 148.8(18) pm in hexafluoro-1,3-butadiene [4] and 147.9(10) and 146.0(20) pm in *trans,trans* and *cis,trans* TME, respectively [5].

An ab initio calculation for 1,3-butadiene has shown that the length of the

TABLE 11

Comparisons of structural parameters for 1,3-butadiene (BUT), and its 2,3-dichloro (D23), *cis,cis*-1,4-dichloro (CC2), *cis,trans*-1,4-dichloro (CT2), *trans,trans*-1,4-dichloro (TT2), *cis,cis*-1,2,3,4-tetrachloro (ZZ4), *trans,trans*-1,2,3,4-tetrachloro (EE4) and the hexachloro (HEX) derivatives; and ethene and its monochloro (MCl), *cis*-dichloro (DCl/C) *trans*-dichloro (DCl/T) and the tetrachloro (TCl) derivatives

		C–C	C=C	C1–Cl	C2–Cl	C=C–C	C=C1–Cl	C3–C2–Cl	ϕ
BUT[b]	[39]	146.3(3)	134.1(2)	–		123.3(5)	–		180
D23	[1]	147.2(4)	133.7(2)	–	174.5(2)	126.1(2)	–	115.2(3)	180
CC2	[2]	145.6(4)	134.3(2)	173.2(3)		125.1(3)	123.7(2)		180
CT2c	[38]	145.6(4)	134.1(2)	172.4(2)		125.6(6)	123.9(3)		180
t			–	–		122.0(6)	122.9(4)		180
TT2	[38]	145.2(5)	134.1(2)	172.4(2)		121.9(6)	122.7(3)		180
ZZ4	[6][c]	149.2(11)	133.6(16)	171.5(11)	170.5(11)	121.7(10)	121.3(8)	116.3(8)	180
EE4[d]		148.1(8)	134.3(5)	172.5(3)	172.5(3)	125.7(4)	122.4(5)	115.6(4)	76.6(23)
HEX[d]		148.5(9)	134.1(5)	171.6(3)	171.6(3)	122.6(4)	122.50(10)	115.8(4)	89(3)
ETH	[40]		133.6(2)						
MCl	[41][e]		134.1(5)	173.0(4)			122.2(5)		
DCl/C	[31]		134.5(6)	171.6(4)			123.8(2)		
DCl/T	[30]		133.5(6)	172.6(4)			120.7(3)		
TCl	[42]		135.4(3)	171.8(3)			122.2(3)		

[a]Distances (r_a) in pm, angles in degrees.
[b]$r_{\alpha}{}^{0}$-values.
[c]XR-investigation, distance type probably close to r_{α}.
[d]This work; all C–Cl bonds assumed to be of equal length. In HEX there are two types of C=C1–Cl but Δ(C=C1–Cl) was negligible.
[e]r_g-values.

C=C bond is rather invariant to changes in the torsional angle and that the C–C bond length is only slightly affected, the r(C=C) and r(C–C) values being respectively 132.0 and 146.3 pm for $\phi = 180°$ and 131.6 and 148.4 pm for $\phi = 90°$ [45] thus supporting the experimental results. However, the controversial question about the relative importance of various contributions to the C–C bond shortening as summarized elsewhere [46], remains unanswered.

ACKNOWLEDGEMENTS

We are grateful to cand. real. Arne Almenningen for recording the electron diffraction diagrams and to Mrs. Snefrid Gundersen for densitometering the photographic plates.

REFERENCES

1 K. Hagen, K. Hedberg, J. Neisess and G. Gundersen, J. Am. Chem. Soc., 107 (1985) 341.
2 G. Gundersen, F. Karlson, Z. Smith and H.G. Thomassen, Acta Chem. Scand. Part A, 40 (1986) 522.
3 G. Gundersen, J. Am. Chem. Soc., 97 (1975) 6342.
4 C.H. Chang, A.L. Andreasson and S.H. Bauer, J. Org. Chem., 36 (1971) 920.
5 M. Trætteberg, Acta Chem. Scand., 24 (1970) 2295.
6 Y. Otaka, Acta Crystallogr., Part B, 28 (1972) 342.
7 H.-O. Bödecker, V. Jonas, B. Kolb, A. Mannschreck and G. Köbrich, Chem. Ber., 108 (1975) 3497, and references therein.
8 G. Becher, T. Burgemeister, H.-H. Henschel and A. Mannschreck, Org. Magn. Reson., 11 (1978) 481.
9 N.A. Zorin, R. Aroca Muños, Yu. N. Panchenko and Yu. A. Pentin, Moscow Univ. Chem. Bull., 28 No. 5 (1973) 20.
10 Yu. N. Panchenko, O.E. Grikina, V.I. Mochalov, Yu. A. Pentin, N.F. Stepanov, R. Aroca, J. Mink, A.N. Akopyan, A.V. Rodin and V.K. Matveev, J. Mol. Struct., 49 (1978) 17.
11 G. Köbrich and H. Büttner, Tetrahedron, 25 (1968) 883.
12 O. Bastiansen, O. Hassel and E. Risberg, Acta Chem. Scand., 9 (1955) 232.
13 K. Tamagawa, T. Iijima and M. Kimura, J. Mol. Struct., 30 (1976) 243, and references therein.
14 A. Borg, Z. Smith, G. Gundersen and P. Klæboe, Spectrochim. Acta, Part A, 36 (1980) 119.
15 E. Benedetti, M. Aglietto, P. Vergamini, R. Aroca Muñoz, A.V. Rodin, Yu. N. Panchenko and Yu. A. Pentin, J. Mol. Struct., 34 (1976) 21.
16 G. Gundersen, P. Klæboe, A. Borg and Z. Smith, Spectrochim. Acta, Part A, 36 (1980) 843.
17 D.A.C. Compton, W.D. George, J.E. Goodfield and W.F. Maddams, Spectrochim. Acta, Part A, 37 (1981) 147.
18 J.P. Toth and D.F. Koster, Spectrochim. Acta, Part A, 31 (1975) 1891.
19 B. Andersen, H.M. Seip, T.G. Strand and R. Stølevik, Acta Chem. Scand., 23 (1969) 3224.
20 A.C. Yates, Comput. Phys. Commun., 2 (1971) 175.
21 T.G. Strand and R.A. Bonham, J. Chem. Phys., 40 (1964) 1686.
22 R.F. Stewart, E.R. Davidson and W.T. Simpson, J. Chem. Phys., 42 (1965) 3175.
23 L. Hedberg, 5th Austin Symposium on Gas Phase Molecular Structure, Austin, Texas, 1974, p. 37.
24 H.M. Seip, T.G. Strand and R. Stølevik, J. Chem. Phys., 3 (1969) 617.

25 L. Hedberg, ASYM20, A Normal Coordinate Computer Program, Oregon State University.
26 K. Kuchitsu, Bull. Chem. Soc. Jpn., 40 (1967) 505.
27 K. Kuchitsu and S.J. Cyvin, in S.J. Cyvin (Ed.), Molecular Structure and Vibration, Elsevier, Amsterdam, 1972, Ch. 12.
28 M. Iwasaki and K. Hedberg, J. Chem. Phys., 36 (1962) 2961.
29 K. Hagen and K. Hedberg, J. Am. Chem. Soc., 95 (1973) 1003.
30 K. Hagen, R. Stølevik and Ø. Thingstad, J. Mol. Struct., 78 (1982) 313.
31 L. Schäfer, J.D. Ewbank, K. Sians, D.W. Paul and D.L. Monts, J. Mol. Struct., 145 (1986) 135.
32 K. Hagen and R. Stølevik, J. Mol. Struct., 147 (1986) 341.
33 O. Bastiansen and S. Samdal, J. Mol. Struct., 128 (1985) 115, and references therein.
34 R. Stølevik and Ø. Thingstad, J. Mol. Struct. (Theochem), 106 (1984) 333.
35 R. Stølevik, J. Mol. Struct. (Theochem), 109 (1984) 397.
36 R. Stølevik, personal communications.
37 P.J. Stavnebrekk and R. Stølevik, J. Mol. Struct., 159 (1987) 153.
38 G. Gundersen, Z. Smith and H.G. Thomassen, Acta Chem. Scand., submitted for publication.
39 K. Kuchitsu, T. Fukuyama and Y. Morino, J. Mol. Struct., 1 (1967-68) 463.
40 K. Kuchitsu, J. Chem. Phys., 44 (1966) 906.
41 P.A.G. Huisman and F.C. Mijlhoff, J. Mol. Struct., 59 (1979) 149.
42 T.G. Strand, Acta Chem. Scand., 21 (1967) 211.
43 K. Kuchitsu, J. Chem. Phys., 49 (1968) 4456.
44 K. Kveseth, Acta Chem. Scand. Part A, 28 (1974) 482.
45 S. Skaarup, J.E. Boggs and P.N. Skancke, Tetrahedron, 32 (1976) 1179.
46 C. Zhixing, J. Mol. Struct. (Theochem), 136 (1986) 57.